Design Equations for the Reflectivity of Deep-Etch Distributed Bragg Reflector Gratings

K. J. Kasunic

***Abstract*—This paper reports a computationally efficient, grid-independent method for calculating the reflectivity of deep-etch distributed Bragg reflector (DBR) gratings. The method employs Gaussian beam propagation in conjunction with a Fabry–Perot model that includes the effects of multiple reflections in multiple cavities. We include both grating pitch and number of Bragg pairs in our analysis. We obtain very good agreement with results generated by a Helmholtz equation solver.**

***Index Terms*—Distributed Bragg reflector (DBR) lasers, gratings, numerical modeling, optical diffraction, optical reflection, optical waveguide components, optoelectronic devices, semiconductor lasers.**

I. Introduction

As a result of recent interest in one-dimensional (1-D) photonic bandgap (PBG) structures [1], [2] and low-threshold edge-emitting lasers for photonic integrated circuit applications [1]–[5], deep-etch distributed Bragg reflectors (DBR's) have been used in various configurations. Consisting of semiconductor/air layers, these gratings have a large index contrast, resulting in high reflectivity over a large wavelength and angular range with few grating pairs. Unfortunately, the evaluation of the reflectivity of these structures currently requires the use of an electromagnetic Maxwell equation solver such as the finite-difference (FD) model employed by Jambunathan and Singh [4]. These solvers typically require significant computational resources; they are further limited by grid size and spacings as to maximum grating pitch and number of grating pairs. The purpose of this paper is to report a computationally efficient, grid-independent method for calculating the reflectivity of deep-etch DBR gratings. Our method allows the rapid evaluation of different design configurations, including the effects of wavelength, modal field size, grating pitch, and number of grating pairs.

II. Theory

We model the geometry shown in Fig. 1, where a slab-waveguide semiconductor laser is fabricated with a deep-etch Bragg grating on one end. Our analysis employs Gaussian beam propagation in conjunction with a Fabry–Perot model that includes the effects of multiple reflections in multiple cavities. Specifically, we first calculate the reflected field due to a DBR grating using classical plane wave techniques [6]. To account for diffractive beam expansion from the waveguide, we then decompose the resulting field into components based on propagation distance. This allows a calculation of Gaussian beam size, which we use in an overlap integral to obtain the coupling efficiency for each component reflected back into the waveguide. The modal reflectivity is a function of the sum of each coupling term multiplied by its associated field component.

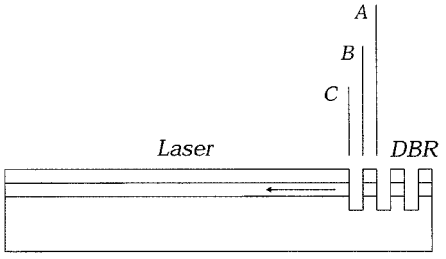

Fig. 1. Schematic of the deep-etch DBR grating, including a slab-waveguide semiconductor laser with modal field radius w_{10}. Surface A is the second surface of the tooth used in (1), surface B is the first surface of the tooth (and the second surface of the gap), and surface C is the first surface of the gap. A wave of unity amplitude is incident on surface C from the left, and is reflected (as shown by the arrow) with amplitude r_b.

To illustrate our approach, we consider a deep-etch Bragg grating consisting of semiconductor teeth with index n_s and gaps (typically) consisting of air with index n_a (Fig. 1). We use the specific example of a single-mode waveguide with field radius w_{10} reflected by a Bragg pair consisting of one gap and one tooth. Excluding diffraction and waveguide coupling, the reflected amplitude u due to the *second* surface in the tooth is given by [6]

$$u = \sum_{m=1}^{\infty} (1-b^2)a^m(-b)^{m-1}e^{im\delta} \tag{1}$$

where m is a counter for the number of multiple reflections included in the single Fabry–Perot cavity formed by the tooth, $\delta = 2k_o n_s d_s$ is the phase shift incurred for an on-axis ray for one round-trip of a tooth with thickness d_s, $a = (n_s - n_a)/(n_s + n_a)$ is the Fresnel reflection coefficient at the semiconductor $\rightarrow$ air interface (surfaces A and C in Fig. 1), and b is the Fresnel coefficient at the air $\rightarrow$ semiconductor interface (surface B). Note that, to later include diffraction effects, we do not use the well-known analytic sum for (1). Also note that, for more than 1 Bragg pair, this formulation allows the use of unique indices for each pair. The field reflectance r_a of an isolated tooth is then given by

$$r_a = b + u \tag{2}$$

Manuscript received June 15, 1999; revised November 15, 1999.

The author was with Sandia National Laboratories, Albuquerque, NM 87185 USA. He is now with the Department of Mathematics, University of Arizona, Tucson, AZ 85721 USA.

Publisher Item Identifier S 0733-8724(00)02198-8.

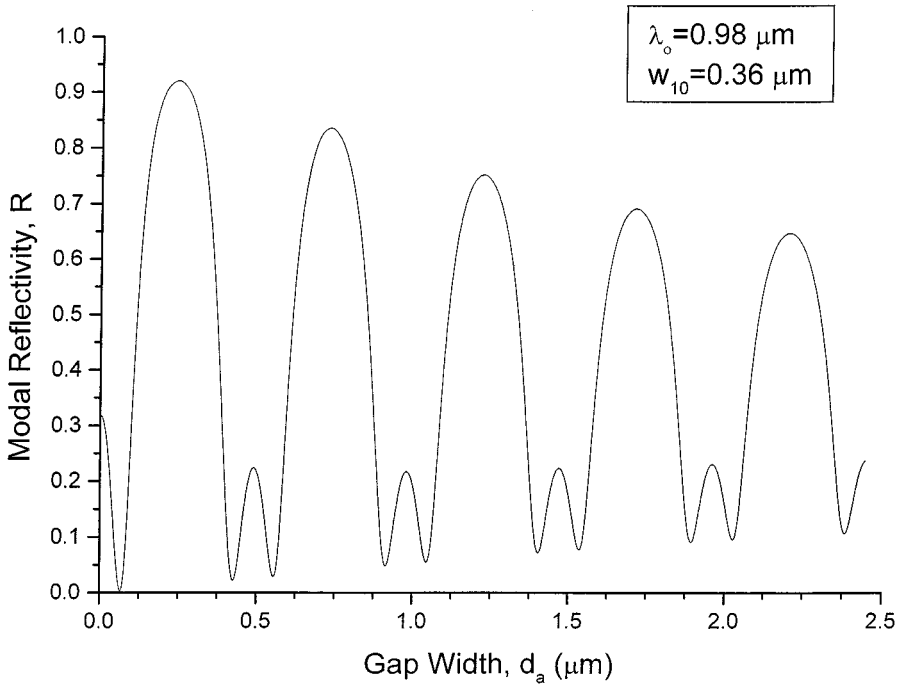

Fig. 2. Modal reflectivity R as a function of gap width d_a for one grating pair (gap and tooth). Refractive indices are $n_{\text{eff}} \equiv n_s = 3.6$ and $n_a = 1.0$, the field radius $w_{10} = 0.36$ μm, and the free-space wavelength $\lambda_o = 0.98$ μm.

from which the reflectivity $R_a = |r_a|^2$ is obtained. To include the effects of the air gap, we first interpret r_a as the equivalent Fresnel coefficient of the second surface of the gap. The reflected amplitude v due to the gap's second surface is therefore [6]

$$v = \sum_{m=1}^{\infty} (1-a^2) r_a^m (-a)^{m-1} e^{im\delta} \tag{3}$$

giving the reflectivity $R_b = |r_b|^2 = |a+v|^2$ for one Bragg pair. We see that, even by truncating the sums in (1) and (3) to 10 terms or so, the effect of multiple reflections in multiple cavities is to quickly increase the number of terms which will be included in (3). Note that the phase thickness δ in the gap is the same as that in the tooth, as typically occurs for gratings fabricated with order $p = 1, 3, 5$, etc.

This procedure can be repeated for an arbitrary number of half-pairs. To include another tooth, for example, we use r_b (rather than r_a) in (3) as the reflectivity of the second tooth surface (and substitute b for a) in the calculation of a third amplitude w. The reflectivity R_c is then given by $|b+w|^2$. Likewise, a fourth Fabry–Perot cavity (in the form of a gap) can be included using r_c in the field summation, and making sure to take into account the alternating a-b sequence.

To account for diffractive effects, we first decompose (3) into it's individual components based on phase

$$v = \sum_{m=1}^{\infty} v_m = \sum_{m=1}^{\infty} C_{v,m} e^{im\delta} \tag{4}$$

with real coefficients $C_{v,m}$ for the mth-component of (3). The modal reflectivity $R = |y|^2$ is then given by the sum of each reflected component multiplied by it's efficiency $\sqrt{\eta_m}$ [7], [8] in coupling back into the waveguide

$$y = a + \sum_{m=1}^{\infty} v_m \sqrt{\eta_m}. \tag{5}$$

A similar procedure has been followed by Karioja and Howe [9] and Sidorin and Howe [10] for the case of a single Fabry–Perot cavity formed by the air gap in extremely-short external cavity (ESEC) lasers. Their methods, however, do not decompose the field as in (4), and are thus not applicable to the case of multiple cavities such as the deep-etch DBR.

To obtain expressions for the η_m, we note that due to the linear relation between δ and d_s (or d_a), the decomposition in (4) allows us to use the well-known Gaussian-beam formula for the field radius w_{1m} of each component [11]

$$w_{1m} = w_{10}\sqrt{1 + \left(\frac{mz\lambda_o}{\pi w_{10}^2}\right)^2} \tag{6}$$

where λ_o is the free-space wavelength and $z = d_{s,a} = \delta\lambda_o/4\pi n_{s,a}$ is the physical thickness of either the tooth or gap associated with a phase thickness of δ. A useful simplification in our model is the use of n_a for all m. As shown below, this results in small errors for the present case of high index contrast between tooth and gap, as $d_s \ll d_a$ for a given δ.

From (6), we obtain the power coupling efficiency for each component [7]

$$\eta_m = \frac{\eta_{0m}}{\sqrt{1+\gamma_m}} \tag{7}$$

where we clearly can assume a transverse displacement $\Delta = 0$ between waveguides, γ_m incorporates the effects of Gaussian

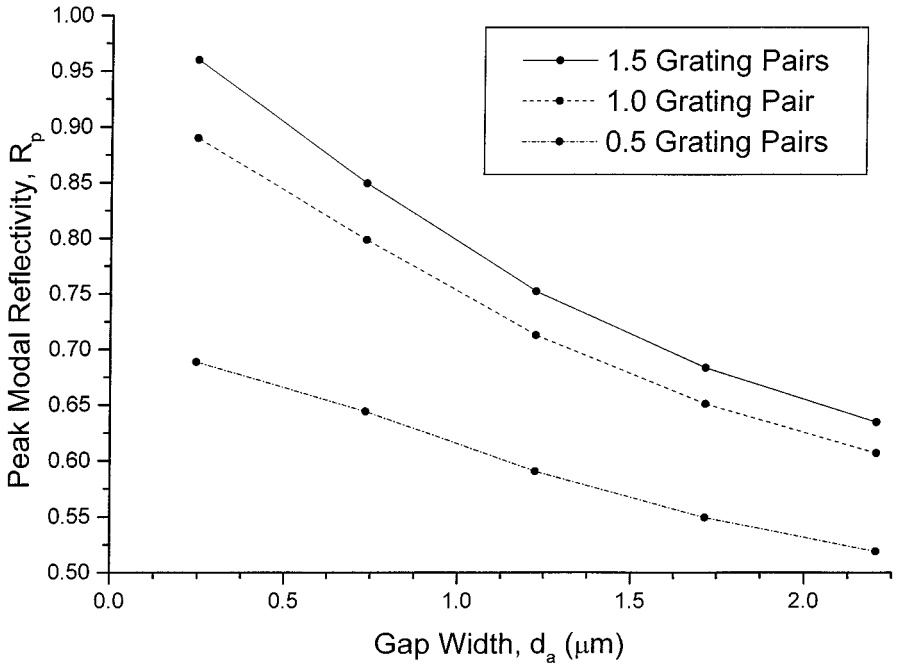

Fig. 3. Peak modal reflectivity R_p as a function of gap width for number of grating pairs = 0.5, 1.0, and 1.5. Each filled dot corresponds to an odd-integer multiple ($p = 1, 3, 5 \ldots$) of quarter-wavelengths in air. The lines connecting the points are merely to show trends for the peaks, and do not imply a continuity of results between points. Except for $n_s = 3.269$, all conditions are the same as in Fig. 2. The plane-wave results (not shown) are horizontal lines with $R_p = 0.965, 0.892$, and 0.687 for 1.5, 1.0, and 0.5 grating pairs, respectively.

beam curvature [see [7], (7)], and η_{0m} is the power coupling efficiency in the absence of curvature effects [7]

$$\eta_{0m} = \frac{2w_{1m}w_{20}}{w_{1m}^2 + w_{20}^2} \tag{8}$$

where $w_{20} = w_{10}$ as we are coupling back into the same waveguide.

III. Results and Discussion

We have used (1)–(8) to calculate the modal reflectivity of various deep-etch DBR structures, including the effects of grating pitch, number of grating pairs, wavelength, and modal field radius. Our results for grating pitch are shown in Fig. 2, where the modal reflectivity is plotted as a function of gap width d_a for the case of 1 Bragg pair and an input wave of magnitude unity. The results clearly show the periodic peaks occuring at gap widths corresponding to odd-integer multiples $p = 1, 3, 5$, etc., of one-quarter of the free-space wavelength $\lambda_o = 0.98\ \mu$m. In the absence of diffraction losses (all $\eta_m = 1.0$), these results match exactly those obtained using, for example, 2×2 matrix techniques [12]. As expected, the inclusion of diffraction reduces the modal reflectivity as d_a increases. Also of interest is the *increase* in the minimum reflectivity for large gaps. While not shown in the figure, our grid-independent method allowed us to verify that these two trends converge at very large d_m to a reflectivity of 32%, corresponding to the Fresnel coefficient at the air/semiconductor interface. This is clearly due to the very weak coupling of the reflected fields back into the waveguide mode.

The peak values of Fig. 2 are replotted in Fig. 3 along with the peak reflectivities for the cases of a single air gap (0.5 grating pairs) and a gap/tooth/gap (1.5 grating pairs) configuration. The figure clearly shows the trend toward higher reflectivity as we increase the number of 1/2-pairs. An interesting feature of the plots is how quickly the reflectivity saturates with number of pairs. Also note that there are differences between our results and those shown in Fig. 2 of [4]. Because of the fixed phase thickness of the teeth used by Jambunathan and Singh, a direct comparison can only be made for the $p = 5$ case. Nevertheless, we obtain substantially higher reflectivities with our model, which we have independently verified (see Table I) with a two-dimensional (2-D) Helmholtz solver [13]. This verification is expected, as the first-order Gaussian beam we use is an analytical solution to the scalar Helmholtz equation in the paraxial approximation. It is not clear why the time-dependent envelope method of [4] gives different results.

The effects of mode size and wavelength are shown in Fig. 4 for the case of one grating pair. The figure shows the expected decrease in reflectivity for smaller mode sizes (longer wavelengths), for which diffractive beam expansion reduces the coupling back into the waveguide mode. For the extreme case of $w_{10}/\lambda \approx 0$, the reflectivity reduces to 32%. This is not shown in the results given in Fig. 4 of [3]. Our figure also shows the asymptotic approach to the plane wave reflectivity of 92% for large mode sizes. The small amount of overshoot seen near $2w_{10}/\lambda = 1.4$ for the $p = 3$ grating is numerical error ($\approx 0.1\%$) associated with truncation of the summation in (1) and (3) to ten terms.

All results shown here were obtained using *Mathematica*, though other approaches are certainly possible. Sources of error in our calculations are threefold. First, we truncate the

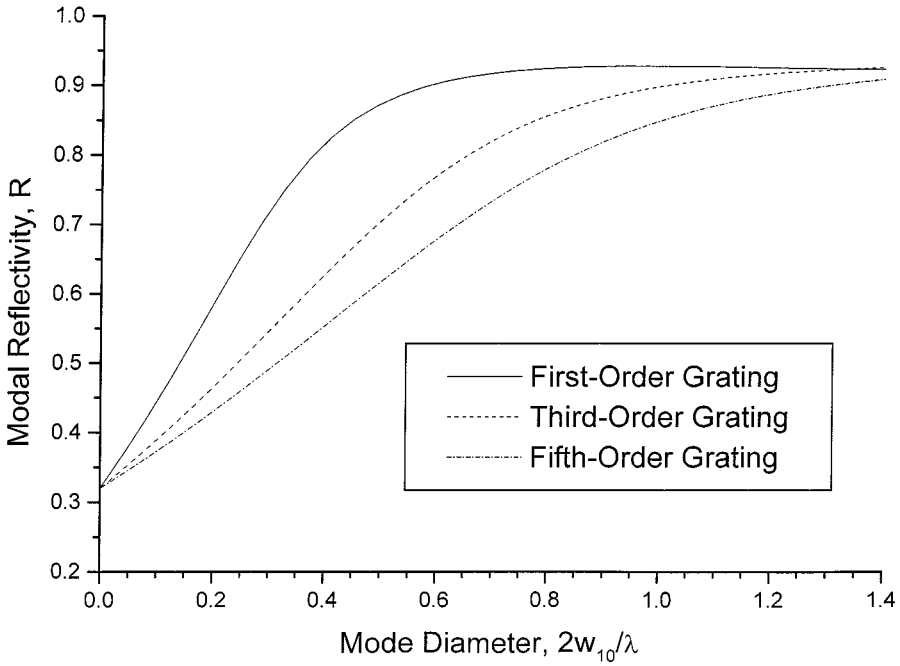

Fig. 4. Modal reflectivity R as a function of mode diameter. The refractive indices, w_{10}, and λ_o are the same as in Fig. 2.

TABLE I
COMPARISON OF R_p FOR GAUSSIAN BEAM MODEL AND HELMHOLTZ SOLVER

p	Gaussian	Helmholtz
1	0.890	0.904
3	0.798	0.822
5	0.713	0.712
7	0.651	0.651
9	0.607	0.607

number of terms included in (1), (3), and (5). Second, the mode size w_{1m} for the mth reflection is typically larger than allowed by the grating depth. That is, a mode size may be on the order of 10 μm after multiple reflections through the cavities. For a first-order grating, on the other hand, with a gap width of 0.25 μm and depth-to-width ratio of approximately 10, some light will not be reflected back to the laser. Fortunately, the remaining field amplitude is small for these reflections, thus resulting in small error. Finally, the approximation used with (6) results in an overestimate of the beam size, and thus an underestimate of the reflectivity. As shown in Table I, our Helmholtz model indicates that numerical errors due to all sources are on the order of 3% ($R = 0.822$ versus 0.798 for $p = 3$) for the conditions of Fig. 3. A comparison with experimental results will also reveal other sources of error, including scattering losses from rough surfaces, the effects of tooth curvature, and other manufacturing imperfections.

IV. CONCLUSION

This paper shows the development of a computationally efficient, grid-independent method for calculating the reflectivity of deep-etch DBR gratings. Our analysis employs Gaussian beam propagation in conjunction with a Fabry–Perot model that includes the effects of multiple reflections in multiple cavities. We envision our technique to be useful for a rapid evaluation of diffraction losses for low-order gratings, as it is a simple matter to modify the refractive indexes, wavelength and modal field radius to examine these effects. This paper obtains very good agreement with results generated by a Helmholtz equation solver.

ACKNOWLEDGMENT

The author appreciates assistance with the Helmholtz solver calculations from G. R. Hadley of Sandia National Laboratories, as well as useful discussions with G. A. Vawter and J. R. Wendt of Sandia National Laboratories, and J. Turner-Valle and T. Valle at Ball Aerospace.

REFERENCES

[1] T. F. Krauss, B. Vogele, C. R. Stanley, and R. M. De La Rue, "Waveguide microcavity based on photonic microstructures," *IEEE Photon. Technol. Lett.*, vol. 9, pp. 176–178, Feb. 1997.

[2] T. F. Krauss, O. Painter, A. Scherer, J. S. Roberts, and R. M. De La Rue, "Photonic microstructures as laser mirrors," *Opt. Eng.*, vol. 37, no. 4, pp. 1143–1147, 1998.

[3] T. Baba, M. Hamasaki, N. Watanabe, P. Kaewplung, A. Matsutani, T. Mukhaihara, F. Koyama, and K. Iga, "A novel short-cavity laser with deep-grating distributed Bragg reflectors," *Jpn. J Appl. Phys.*, vol. 35, no. 2B, pp. 1390–1394, 1996.

[4] R. Jambunathan and J. Singh, "Design studies for distributed Bragg reflectors for short-cavity edge-emitting lasers," *IEEE J. Quanum. Electron.*, vol. 33, pp. 1180–1189, July 1997.

[5] Y. Yuan, T. Brock, P. Bhattacharya, C. Caneau, and R. Bhat, "Edge-emitting lasers with short-period semiconductor/air distributed Bragg reflector mirrors," *IEEE Photon. Technol. Lett.*, vol. 9, pp. 881–883, July 1997.
[6] D. L. Caballero, "A theoretical development of exact solutions of multiple layer optical coatings," *J. Opt. Soc.*, vol. 37, no. 3, pp. 176–180, 1947.
[7] D. G. Hall, R. R. Rice, and J. D. Zino, "Simple gaussian-beam model for GaAlAs double-heterostructure laser-diode-to-diffused-waveguide coupling calculations," *Opt. Lett.*, vol. 4, no. 9, pp. 292–294, 1979.
[8] D. G. Hall, J. D. Spear-Zino, H. G. Koenig, R. R. Rice, J. K. Powers, G. H. Burkhart, and P. D. Bear, "Edge coupling of a GaAlAs DH laser diode to a planar Ti:$LiNbO_3$ waveguide," *Appl. Opt.*, vol. 19, no. 11, pp. 1847–1852, 1980.
[9] P. Karioja and D. Howe, "Diode-laser-to-waveguide butt coupling," *Appl. Opt.*, vol. 35, no. 3, pp. 404–416, 1996.
[10] Y. Sidorin and D. Howe, "Laser-diode wavelength tuning based on butt coupling into an optical fiber," *Opt. Lett.*, vol. 22, no. 11, pp. 802–804, 1997.
[11] A. E. Siegman, *Lasers*. Mill Valley, CA: University Science Books, 1986, ch. 17.
[12] M. Mansuripur, "Analysis of multilayer thin-film structures containing magneto-optic and anistropic media at oblique incidence using 2×2 matrices," *J. Appl. Phys.*, vol. 67, no. 10, pp. 6466–6475, 1990.
[13] G. R. Hadley, "Numerical simulation of reflecting structures by solution of the two-dimensional Helmholtz equation," *Opt. Lett.*, vol. 19, no. 2, pp. 84–86, 1994.

K. J. Kasunic, photograph and biography not available at the time of publication.